mathematics

MDPI

Article

Predicting the Dynamic Response of Dual-Rotor System Subject to Interval Parametric Uncertainties Based on the Non-Intrusive Metamodel

Chao Fu [1,2], Guojin Feng [2], Jiaojiao Ma [2,3], Kuan Lu [1,*], Yongfeng Yang [1] and Fengshou Gu [2]

[1] Institute of Vibration Engineering, Northwestern Polytechnical University, Xi'an 710072, China; fuchao0606@mail.nwpu.edu.cn (C.F.); yyf@nwpu.edu.cn (Y.Y.)
[2] Centre for Efficiency and Performance Engineering, University of Huddersfield, Queensgate, Huddersfield HD1 3DH, UK; G.Feng@hud.ac.uk (G.F.); J.Ma@hud.ac.uk (J.M.); F.Gu@hud.ac.uk (F.G.)
[3] School of Mechanical Engineering, Hebei University of Technology, Tianjin 300401, China
* Correspondence: lukuan@nwpu.edu.cn

Received: 12 April 2020; Accepted: 3 May 2020; Published: 7 May 2020

Abstract: In this paper, the non-probabilistic steady-state dynamics of a dual-rotor system with parametric uncertainties under two-frequency excitations are investigated using the non-intrusive simplex form mathematical metamodel. The Lagrangian formulation is employed to derive the equations of motion (EOM) of the system. The simplex form metamodel without the distribution functions of the interval uncertainties is formulated in a non-intrusive way. In the multi-uncertain cases, strategies aimed at reducing the computational cost are incorporated. In numerical simulations for different interval parametric uncertainties, the special propagation mechanism is observed, which cannot be found in single rotor systems. Validations of the metamodel in terms of efficiency and accuracy are also carried out by comparisons with the scanning method. The results will be helpful to understand the dynamic behaviors of dual-rotor systems subject to uncertainties and provide guidance for robust design and analysis.

Keywords: dual-rotor; multi-frequency excitation; non-intrusive calculation; metamodel

1. Introduction

Risk analyses and optimization of engineering mechanical systems always play an important role in the design and maintenance [1,2]. To optimize and improve the dynamic performance, a dual-rotor system is widely employed in modern aero-engines for large surge margin. It is more complicated than single rotor systems in both the structural and dynamical regimes. Researchers have paid attention to the vibrations of dual-rotors under faults, such as the imbalance and rub-impact [3–5]. The design and modeling of dual-rotors were also intensively studied over the past few decades [6–9]. The application of rotor-bearing structures in the dual-rotor systems were investigated both theoretically and experimentally [10]. To improve the fidelity, the differences between 1D and 3D models of dual-rotor systems were studied [11].

The reported contributions provide guidance for the dynamical assessments of dual-rotor systems. However, an important feature of practical engineering mechanical systems has been ignored, which is that the physical parameters of the models and working conditions will behave in an uncertain way inherently [12–15]. For a complex engineering dual-rotor system, this problem will be more prominent. In recent literature [16–19], the sources and causes of parametric uncertainties in rotor systems were explained in detail, especially the complex stiffness of the connecting structures. It is gradually recognized that the inherent uncertainty should not be overlooked for robust design and dynamic behaviors prediction. Efforts have already been made to investigate the effects of uncertainties

in rotor dynamical systems. The polynomial chaos expansion in combination of the harmonic balance method was used to quantify the effects of different random parametric uncertainties on the linear and non-linear dynamical characteristics [20–22]. More recently, the Kriging metamodeling was applied to the prediction of uncertain behaviors of flexible rotor systems [17]. The nonparametric modeling [14] was also introduced into the uncertainty quantification for a Jeffcott rotor [23] as well as analyses in terms of the balancing and unbalancing [24]. Considering the random excitations, the power spectral density of the unbalance response of an aero-engine dual-rotor was analyzed in [25]. The modeling and stochastic frequency response functions of rotors subject to random uncertainties were studied by using the Karhunen–Loève decomposition [26].

As can be observed, the widely adopted and employed uncertainty analysis methods mostly belong to the probabilistic domain. In practical situations, it is generally difficult or too expensive to gather enough prior data for the uncertain parameters. The interval analysis procedures are more versatile and easier to implement due to their non-probabilistic characteristics [13]. The Chebyshev inclusion function proposed by Wu et al. [27] has attracted wide attention in the past few years due to its simplicity in concept and non-intrusiveness. Several improved forms have been developed and applied to uncertain mechanical systems [28,29]. Although the interval analysis has been widely used in structural dynamics of the truss and multibody systems, it has not been applied to the uncertain rotor dynamics until recent years [30,31]. Some meaningful results have been obtained in these contributions using the interval models. However, formulations and applications of metamodeling methodologies based on non-probabilistic descriptions have not attracted sufficient attention. The computational burden needs also to be reduced. The vibration characteristics of dual-rotor systems subject to multi-frequency excitation and interval variables remain to be revealed.

This paper presents the non-intrusive metamodeling for the uncertainty quantification of a dual-rotor system. The major purposes are to calculate the steady-state dynamic responses of such a system under interval uncertainties and illustrate the effectiveness of the metamodel. First, the dual-rotor model and its motion equations will be described in Section 2. Then, in Section 3, the formulation of the metamodel for single and multi-uncertain variables is explained. Next, propagations of uncertainties of different physical parameters are studied and discussed in Section 4. Finally, the concluding remarks are drawn in Section 5.

2. Model Description and Motion Equations

A dual-rotor system often consists of a higher pressure (HP) rotor and a lower pressure (LP) rotor, which are connected by the inter-shaft bearing and rotate at different angular speeds. They can also be referred to as the inner and outer rotors [8,32]. Figure 1 shows the schematic diagram of a typical dual-rotor system. The rotors are mounted on massless shafts and supported by three rigid isotropic bearings with stiffness and damping k_1, c_1 k_2, c_2 and k_3, c_3. The m_1, J_{d1}, J_{p1} and m_2, J_{d2}, J_{p2} are the mass, diameter moment of inertia and polar moment of inertia of the HP and LP rotors, respectively. There are mass imbalances on both of the rotors, denoted by e_1 and e_2. The angular rotating speeds of the LP and HP rotors are ω_1 and ω_2. The span of the system is L and the other locations are measured by their corresponding distances from the left end $L_i, i = 1, 2, 3, 4$, as shown in Figure 1.

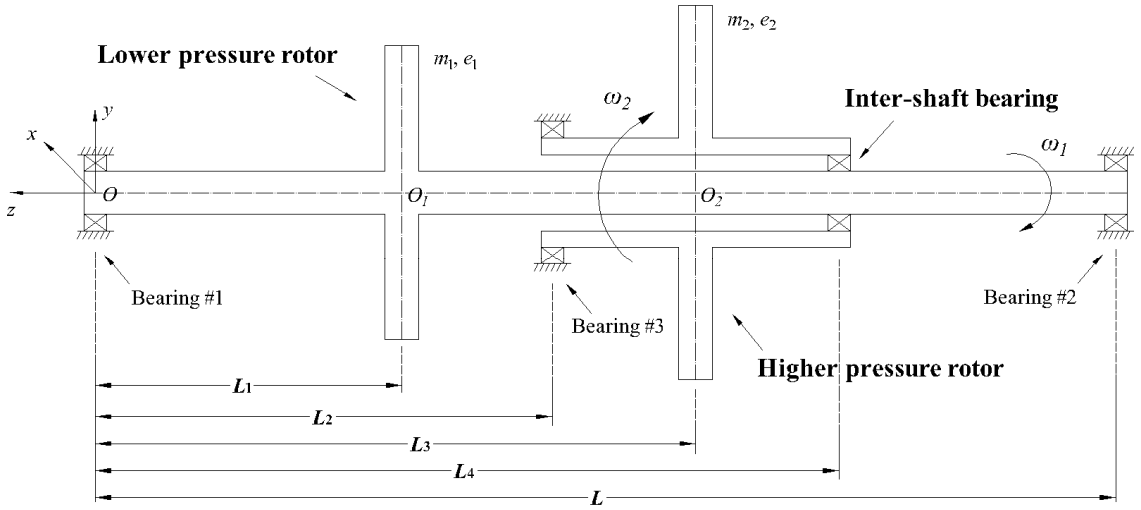

Figure 1. Configuration of a typical dual-rotor system.

The system can be described by eight degrees-of-freedom (DOFs) and four for each rotor, i.e., two lateral displacements and two rotational angles [33,34]. It is obtained as

$$\mathbf{q} = [x_1, y_1, \theta_{y1}, \theta_{x1}, x_2, y_2, \theta_{y2}, \theta_{x2}]^T \tag{1}$$

where subscripts 1 and 2 correspond to the LP and HP rotors. After this, the coordinates of the three bearing centers can be derived using the eight basic DOFs

$$\begin{cases} x_{b1} = x_1 - L_1\theta_{y1} \\ y_{b1} = y_1 + L_1\theta_{x1} \end{cases}, \begin{cases} x_{b2} = x_1 + (L - L_1)\theta_{y1} \\ y_{b2} = y_1 - (L - L_1)\theta_{x1} \end{cases}, \begin{cases} x_{b3} = x_2 - (L_3 - L_2)\theta_{y2} \\ y_{b3} = y_2 + (L_3 - L_2)\theta_{x2} \end{cases} \tag{2}$$

Modeling rotating systems based on the energy analyses is widely employed in the community of rotor dynamics [34]. For the system under study, the kinetic energy can be calculated as

$$\begin{cases} T = T_1 + T_2 \\ T_i = \frac{1}{2}m_i(\dot{x}_i^2 + \dot{y}_i^2) + \frac{1}{2}J_{di}(\dot{\theta}_{xi}^2 + \dot{\theta}_{yi}^2) + J_{pi}\omega_i^2 - J_{pi}\omega_i\dot{\theta}_{yi}\theta_{xi},\ i = 1,\ 2 \end{cases} \tag{3}$$

The potential energy is contributed by the three bearings and can be denoted by

$$\begin{cases} V = V_1 + V_2 + V_3 \\ V_i = \frac{1}{2}k_i(x_{bi}^2 + y_{bi}^2),\ i = 1,\ 2,\ 3 \end{cases} \tag{4}$$

Accordingly, the dissipation energy can be expressed as

$$\begin{cases} D = D_1 + D_2 + D_3 \\ D_i = \frac{1}{2}c_i(\dot{x}_{bi}^2 + \dot{y}_{bi}^2),\ i = 1,\ 2,\ 3 \end{cases} \tag{5}$$

If the connection of the inner and outer rotors are modeled as a linear spring and its stiffness is k_c, the reacting forces of the inter-shaft bearing are as follows

$$\begin{cases} F_x = k_c[x_1 + (L_4 - L_1)\theta_{y1} - x_2 - (L_4 - L_3)\theta_{y2}] \\ F_y = k_c[y_1 - (L_4 - L_1)\theta_{x1} - y_2 + (L_4 - L_3)\theta_{x2}] \end{cases} \tag{6}$$

When rotating, the unbalance forces on the two rotors are obtained by

$$\begin{cases} \mathbf{F}_{u1}(t) = [m_1 e_1 \omega_1^2 \cos(\omega_1 t),\ m_1 e_1 \omega_1^2 \sin(\omega_1 t),\ 0,\ 0,\ 0,\ 0,\ 0,\ 0]^T \\ \mathbf{F}_{u2}(t) = [0,\ 0,\ 0,\ 0,\ m_2 e_2 \omega_2^2 \cos(\omega_2 t),\ m_2 e_2 \omega_2^2 \sin(\omega_2 t),\ 0,\ 0]^T \end{cases} \tag{7}$$

The Lagrangian equation considering dissipation effects can be applied to the system as

$$\frac{\mathrm{d}}{\mathrm{dt}}\left(\frac{\partial T}{\partial \dot{q}_j}\right) + \frac{\partial D}{\partial \dot{q}_j} - \frac{\partial T}{\partial q_j} + \frac{\partial V}{\partial q_j} = Q_j,\ j = 1,\ 2,\ \ldots,\ 8 \tag{8}$$

Submitting Equations (1)–(7) into Equation (8) and rearranging the results into matrix form, the motion equations of the dual-rotor system can be obtained as

$$\mathbf{M}\ddot{\mathbf{q}}(t) + \widetilde{\mathbf{C}}\dot{\mathbf{q}}(t) + \mathbf{K}\mathbf{q}(t) = \mathbf{F}(t) \tag{9}$$

where $\mathbf{M}$ and $\mathbf{K}$ are the mass and stiffness matrices of the system, $\widetilde{\mathbf{C}}$ includes the damping and gyroscopic effects, $\mathbf{F}(t)$ integrates the unbalance forces and the reacting forces in the inter-shaft bearing. A dot over the displacement vector $\mathbf{q}$ denotes derivation with respect to time. The rotational speeds or frequencies of the inner and outer rotors are incommensurable, making Equation (9) a system excited by two frequencies. Its solution can be obtained by numerical methods and the fourth order Runge–Kutta method with variable steps, which will be used in this paper.

3. Non-Intrusive Interval Analysis of the System Based on Meta-Modeling

As a practical problem, the accurate distribution model of the uncertainty is difficult to establish. In other words, the problem is small sample-sized. Therefore, the interval methods may be more suitable to implement. However, the intrusive interval methods need to modify the deterministic solution packages and are complicated in mathematical formulation. The surrogate methods [17,28,30] popular nowadays should be a good choice. These methodologies are simple in deduction and they work in a non-intrusive way because the deterministic dynamic problem can be used as a black box. Importantly, the computational cost of them should be carefully managed to ensure economic and feasible analyses. In this paper, we establish a simplex metamodel for the dynamic responses of the dual-rotor system considering non-probabilistic interval uncertainties. The small-range constraint in the conventional perturbation method is released. Moreover, the surrogates need not to find the gradient direction of parametric uncertainties to track their propagations, which is essential in the Taylor-based interval methods. In the latter, the difficulties in obtaining the high order derivative information will also limit the applications. Without loss of generality, we firstly consider the case where only one interval parameter is included. The interval parameter can be expressed as

$$a^I = [\underline{a},\ \overline{a}] = [a^c - \beta a^c,\ a^c + \beta a^c] \tag{10}$$

where superscript I designates an interval variable, the bars over and under a quantity denote its upper and lower limits. Notations a^c and β are the mid-value and uncertain degree of a^I. An interval character can be completely defined when the lower and upper bounds are given, which are much easier to obtain than the precise probability model. The following relationships can be further obtained

$$\begin{cases} a^c = (\underline{a} + \overline{a})/2 \\ \Delta a = (\overline{a} - \underline{a})/2 \\ \beta = \Delta a / a^c \end{cases} \tag{11}$$

Taking the interval uncertainty into consideration, the motion equations of the dual-rotor system evolve to interval ordinary differential equations (IODEs). Due to the interval input, the system

outputs should also be interval quantities. Consequently, we can rewrite the displacement vector of the dual-rotor system in interval form

$$\mathbf{q}^I(t) = [\underline{\mathbf{q}}(t), \overline{\mathbf{q}}(t)] = \left\{\mathbf{q}(a,\ t)\middle| a \in a^I\right\} \tag{12}$$

Efforts should be taken to find the distribution limits of the uncertain displacements. Direct interval arithmetic will introduce enormous errors which make the results meaningless. Here, we consider Equation (12) as a constraint to the system given in Equation (9) and formulate the metamodel based on the approximation theories. Equation (10) can be written in another form using the standard interval

$$a^I = a^c + \Delta a[-1,\ 1] \tag{13}$$

It is clear that for any possible value of the uncertain parameter $a \in a^I$, we can find an alternative variable $\xi \in [-1,\ 1]$ which is equivalent to it with linear projection. Therefore, this can be used to handle the uncertain problem on the standard interval. The actual value of the uncertain parameter can be obtained using a reverse projection. Therefore, a simplex radial basis is established

$$\Xi = [1,\ \xi, \xi_2,\ \cdots,\ \xi_n, \cdots]^{\mathrm{T}} \tag{14}$$

Based on the polynomial basis, a simplex form metamodel of the uncertain responses of the dual-rotor can be constructed as

$$S(\xi) = \sum_{i}^{\infty} \Upsilon_i \xi^i = \boldsymbol{\Upsilon}\Xi, i = 0,\ 1,\ 2,\ \ldots \tag{15}$$

Equation (15) attempts to approximate the actual uncertain system with the weighted sum of a series of simplex. In practical calculation, it is only possible to consider finite number of terms and we truncate it to k herein. The weight coefficient vector $\boldsymbol{\Upsilon} = \{\Upsilon_i,\ i = 0,\ 1,\ 2,\ \ldots\}$ needs to be determined to fully formulate the metamodel. To this end, samples of the responses of the dual-rotor should be drawn. The roots of orthogonal polynomials are effective sample candidates in the parameter space and they are widely adopted in stochastic and non-probabilistic computations [29,35]. Here, the Chebyshev roots will be used, which can be calculated as

$$\vartheta_i = \cos[\frac{2i-1}{2(k+1)}\pi], i = 1,\ 2,\ \cdots,\ k+1 \tag{16}$$

Subsequently, the sampled responses from the deterministic system can be obtained by simulations of the model with the uncertain parameter specified to the samples and others kept to their mid-values.

$$\widetilde{a}_i = a^c + \beta a^c \vartheta_i, i = 1,\ 2,\ \cdots,\ k+1 \tag{17}$$

$$\widetilde{\mathbf{q}}_i(t) = \left\{\mathbf{q}(a,\ t)\middle| a = \widetilde{a}_i \in a^I\right\},\ i = 1,\ 2,\ \cdots,\ k+1 \tag{18}$$

Subsequently, Equation (15) evolves to

$$\widetilde{\mathbf{q}}(\vartheta) = \boldsymbol{\Upsilon}\widetilde{\Xi}(\vartheta) \tag{19}$$

where $\widetilde{\mathbf{q}}$ and $\widetilde{\Xi}$ are the sample response vector from the dual-rotor and the value matrix of the radius basis vector at uncertainty sample series $\vartheta = \{\vartheta_i\}$, $i = 1,\ 2,\ \cdots,\ k+1$. The $\widetilde{\Xi}$ is expressed as

$$\widetilde{\Xi} = \begin{bmatrix} 1 & \vartheta_1 & \vartheta_1^2 & \cdots & \vartheta_1^k \\ 1 & \vartheta_2 & \vartheta_2^2 & \cdots & \vartheta_2^k \\ \vdots & \vdots & \ddots & \vdots & \vdots \\ 1 & \vartheta_{k+1} & \vartheta_{k+1}^2 & \cdots & \vartheta_{k+1}^k \end{bmatrix} \tag{20}$$

In Equation (19), there are $k+1$ unknown weight coefficients and the number of equations is the same. Thus, the coefficient vector can be directly solved

$$\boldsymbol{\Upsilon} = \widetilde{\mathbf{q}}(\vartheta)[\widetilde{\Xi}(\vartheta)]^{-1} \tag{21}$$

Once the coefficient vector is obtained, the metamodel is fully determined. It is a simplex form function aimed to represent the actual distribution model of the uncertain dynamic response, which has unknown mathematical descriptions. As the lower and upper bounds of the system responses are of interest, the metamodel can be used to derive these values, which should be simple.

For multi uncertain variables, the basic idea is the same but some strategies to reduce the computation cost should be incorporated. For example, in the case that the dual-rotor contains n interval uncertainties, the radius basis vector can be rewritten in ascending order as

$$\Xi = [1,\ \xi_1,\ \cdots,\ \xi_n, \xi_1^2, \xi_1\xi_2,\ \cdots,\ \xi_n^2,\ \cdots,\ \xi_1^k, \xi_1^{k-1}\xi_2,\ \cdots,\ \xi_n^k]^T \tag{22}$$

The number of elements in Ξ is

$$N = \frac{(n+k)!}{n!k!} \tag{23}$$

The metamodel is expressed by the weighted sum of terms whose order is no greater than k

$$S(\xi) = \sum_{0 \le i_1 + \ldots + i_n \le k} \Upsilon_{i_1,\cdots,i_n} \xi_1^{i_1} \xi_2^{i_2} \cdots \xi_n^{i_n} = \boldsymbol{\Upsilon}\Xi, i_1, \cdots, i_n = 0,\ 1,\ \ldots,\ k \tag{24}$$

where $\Upsilon_{i_1,\cdots,i_n}$ is the multi-dimensional coefficient. There will be $(k+1)^n$ samples based on Equation (16) when all the sample candidates are chosen for every uncertain dimension.

In problems with relatively large number of interval parameters, the computation cost will be high. It is demonstrated that when the used samples are twice of the unknowns in the metamodel, the model will be robust and the efficiency is enhanced [36]. In such way, the number of samples kept will be $2N$. The number of unknown coefficients is not the same as that of equations, the least square method can be introduced to evaluate the regression coefficients

$$\boldsymbol{\Upsilon} = \widetilde{\mathbf{q}}(\widetilde{\vartheta})\widetilde{\Xi}(\widetilde{\Xi}^T\widetilde{\Xi})^{-1} \tag{25}$$

where $\widetilde{\mathbf{q}}(\widetilde{\vartheta})$ is the $8 \times 2N$ matrix for the deterministic sample response drawn from the dual-rotor system based on the uncertain parameter sample sets

$$\begin{cases} \widetilde{\vartheta} = [\vartheta_1,\ \vartheta_2,\ \cdots,\ \vartheta_{2N}] \\ \vartheta_j = \left\{\vartheta_{i,j}\right\}, i = 1,\ 2,\ \cdots,\ n \end{cases} \tag{26}$$

In Equation (26), there are $2N$ sets of samples and each set contains n elements. The matrix $\widetilde{\Xi}$ in Equation (25) represents the values of the radius basis vector calculated at the parameter sample sets

$$\widetilde{\Xi} = \begin{bmatrix} 1 & \vartheta_{1,1} & \cdots & \vartheta_{n,1} & \vartheta_{1,1}^2 & \vartheta_{1,1}\vartheta_{2,1} & \cdots & \vartheta_{n,1}^2 & \cdots & \vartheta_{1,1}^k & \vartheta_{1,1}^{k-1}\vartheta_{2,1} & \cdots & \vartheta_{n,1}^k \\ 1 & \vartheta_{1,2} & \cdots & \vartheta_{n,2} & \vartheta_{1,2}^2 & \vartheta_{1,2}\vartheta_{2,2} & \cdots & \vartheta_{n,2}^2 & \cdots & \vartheta_{1,2}^k & \vartheta_{1,2}^{k-1}\vartheta_{2,2} & \cdots & \vartheta_{n,2}^k \\ \vdots & \vdots & \ddots & \vdots & \vdots & \vdots & \ddots & \vdots & \ddots & \vdots & \vdots & \ddots & \vdots \\ 1 & \vartheta_{1,N} & \cdots & \vartheta_{n,N} & \vartheta_{1,N}^2 & \vartheta_{1,N}\vartheta_{2,N} & \cdots & \vartheta_{n,N}^2 & \cdots & \vartheta_{1,N}^k & \vartheta_{1,N}^{k-1}\vartheta_{2,N} & \cdots & \vartheta_{n,N}^k \end{bmatrix}_{2N\times N} \tag{27}$$

in which the first sub index refers to different uncertain variables and the second to the sample sets expressed in Equation (26). The above deduction is for interval problems involving multiple parametric uncertainties embedded with computational burden alleviation strategies.

When the explicit meta-model is constructed, the bounds of the dynamic response or the extreme values of the meta-model can be easily solved. Since it is in simplex form, the scanning method can be applied to the meta-model to find the bounds efficiently when the dimension of uncertainties is not too high (no greater than three, for example). It can be expressed as

$$\begin{cases} s_i = S(\hat{\xi}_i), i = 1,\ 2,\ \ldots,\ p \\ \underline{\mathrm{q}}(t) = \min([s_1,\ \ldots,\ s_p]), \overline{\mathrm{q}}(t) = \max([s_1,\ \ldots,\ s_p]) \end{cases} \tag{28}$$

where $\hat{\xi}_i$ represents the grid parametric points produced in the scanning and p is the total number of them. If many uncertainties are involved (greater than three), the max/min values of the meta-function should be evaluated by the optimization methods, such as the genetic algorithm [28].

4. Results and Discussions

In this section, numerical simulations of the dual-rotor system based on the previous approaches will be presented. The model has the following values of the physical parameters: $\mathrm{m}_1 = 16.25$ kg, $J_{p1} = 0.134\ \mathrm{kg\cdot m^2}$, $J_{d1} = 0.0698\ \mathrm{kg\cdot m^2}$; $m_2 = 8.4$ kg, $J_{p2} = 0.0793\ \mathrm{kg\cdot m^2}$, $J_{d2} = 0.0405\ \mathrm{kg\cdot m^2}$; $e_1 = 3\times10^{-5}$ m, $e_1 = 8\times10^{-5}$ m; $L_1 = 0.2$ m, $L_2 = 0.24$ m, $L_3 = 0.44$ m, $L_4 = 0.54$ m, $L = 0.62$ m; $c_1 = c_2 = c_3 = 14.69\ \mathrm{N\cdot s/m}$, $k_1 = k_2 = k_3 = 5\times10^6\ \mathrm{N/m}$, $k_b = 8\times10^7\ \mathrm{N/m}$. The rotation speed ratio between the HP and LP rotors is 1.2. In this paper, we use the maximum vibration deflections of the two rotors at every rotating speed for demonstration, which can be calculated as $\max(\sqrt{x_i^2 + y_i^2}),\ i = 1, 2$. The deterministic steady-state dynamic responses of the HP and LP rotors excluding uncertainty are given in Figure 2. It is observed that the first two peaks appear at 738.4 rad/s and 886.1 rad/s for both of the rotors and the amplitudes of the LP rotor are higher than the HP rotor. It should be noted that the simplified model used in the currently study is sufficient for uncertainty propagation analysis and excludes irrelevant factors that may cause response variability. In order to capture detailed natural characteristics, however, sophisticated physical models should be developed for the comprehensive modal analysis of engineering dual-rotor systems. We refer interested readers to [37] for more information. In the next few sections, different physical parameters are considered uncertain and their effects are investigated based on the three-order metamodel.

4.1. Effect of Interval Mass Eccentricity

Firstly, we treat the uncertainties in the two eccentricities on the rotors. In an engineering context, the balancing status often gets worse after assembling the well-balanced rotors. The reason may be the assembly errors and hardness to measure. Moreover, the imbalance can be influenced by material degradation and wear. Therefore, the imbalance or mass eccentricity should be considered uncertain in analysis. We take the uncertain degree to be $\beta = 10\%$. If $e_1 = [2.7,\ 3.3]\times10^{-5}$ m, the interval response can be analyzed using the metamodel established in Section 3 and the results for the LP rotor are plotted in Figure 3. For comparison, the results for uncertain imbalances on the HP rotor

are given in Figure 4 when $e_2 = [7.2,\ 8.8] \times 10^{-5}$ m. To provide a reference for the uncertain effects, the deterministic curves shown in Figure 2 will be added in all the uncertain cases.

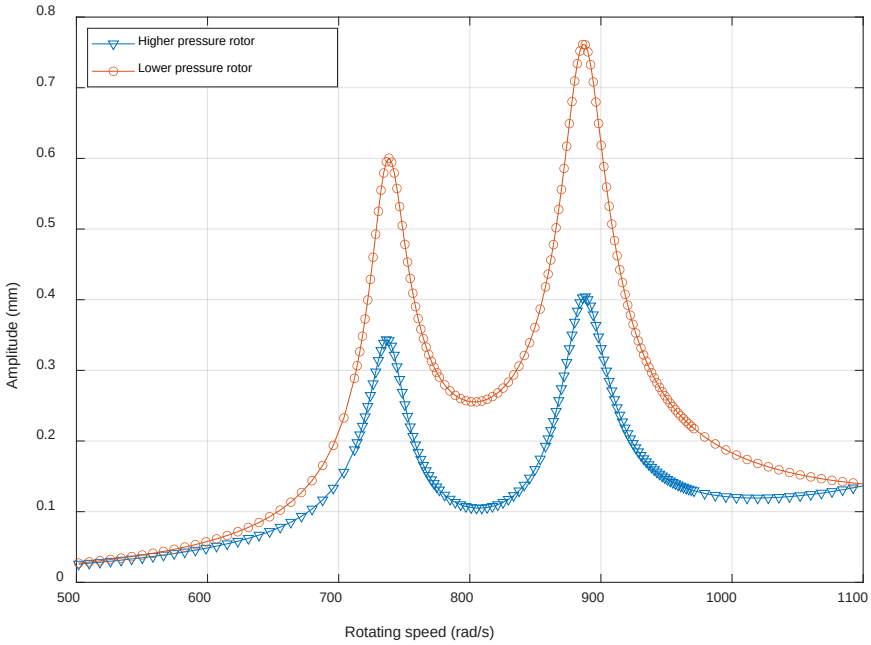

Figure 2. Deterministic steady-state responses of the dual-rotor system.

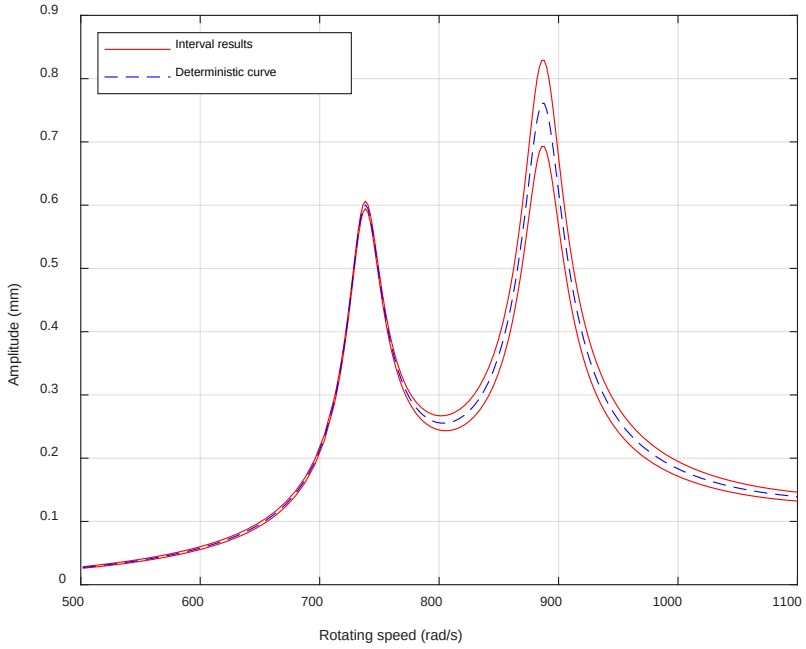

Figure 3. Dynamic response of the Lower Pressure (LP) rotor with uncertain imbalance on the LP rotor.

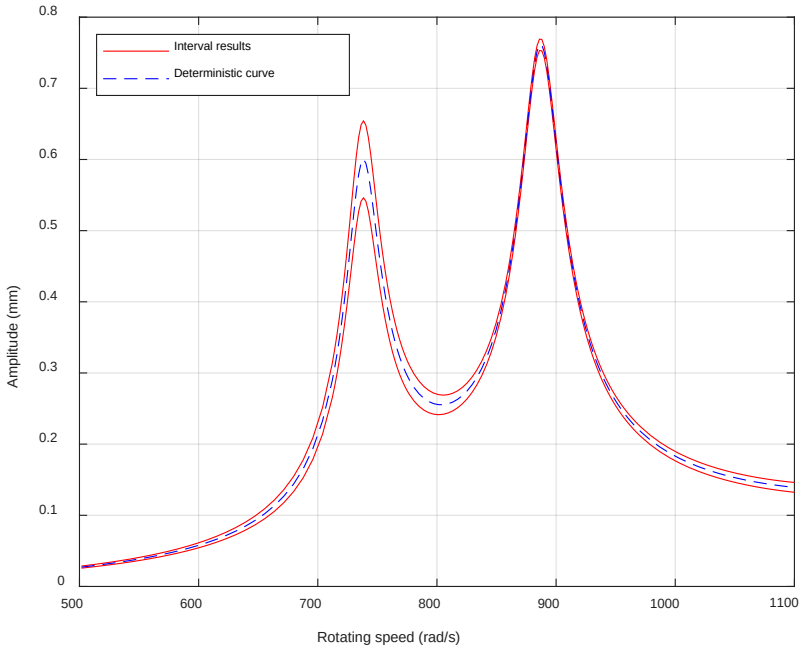

Figure 4. Dynamic response of the LP rotor with uncertain imbalance on the Higher Pressure (HP) rotor.

A major difference between Figures 3 and 4 is that the response interval occurs at different rotation speed bands. Uncertainty in either of the two imbalances will not cause significant deviations of the system responses in the whole speed range. More specifically, the uncertainty in the imbalance on the LP rotor has effects mainly in the speed range around the second peak, while interval imbalance on the HP rotor will influence the first resonance area. That is because the mass imbalances on the two rotors correspond to their respective vibration peaks. Similar characteristics are also found in the parametric investigations of the dual-rotor systems [8]. This phenomenon indicates the different sensitivities of the system in different speed ranges to the two imbalances, which is not observed in single rotor systems. In the respective effective ranges of the two uncertainties, the deterministic response is symmetrically deviated and the enveloped ranges are related to the magnitude of the uncertain degree. Due to the presence of uncertainties, the dynamic response of the system can be any possible values in the response interval.

4.2. Effect of Interval Bearing Stiffness

The stiffness of bearing #1 is taken as an interval quantity to cover its variability [15–18]. Generally, it is difficult to define the accurate value of the stiffness of a support. In this case, the uncertain degree of the interval uncertainty is 5%. Subsequently, the stiffness can be expressed as $k_1 = [4.75,\ 5.25] \times 10^6$ N/m. The response range of the HP rotor is shown in Figure 5.

As can been seen from Figure 5, the uncertain behaviors of the dual-rotor are totally different from the cases with uncertain imbalances. The deterministic response curve is significantly deviated and the lower bound and upper bound are asymmetric. Near the first peak, a slope peak in the upper bound and a sharp one in the lower bound are found. In addition, the positions of the peaks are shifted compared with the deterministic one with the lower to the left and the upper to the right. There is an observable flat band in the upper bound around the second peak. These features are introduced by the alterations in the intrinsic characteristics caused by the uncertainty. The results also prove that the dual-rotor is sensitive to the support stiffness of bearing #1. It may be considered a key factor for design and maintenance of such engineering systems.

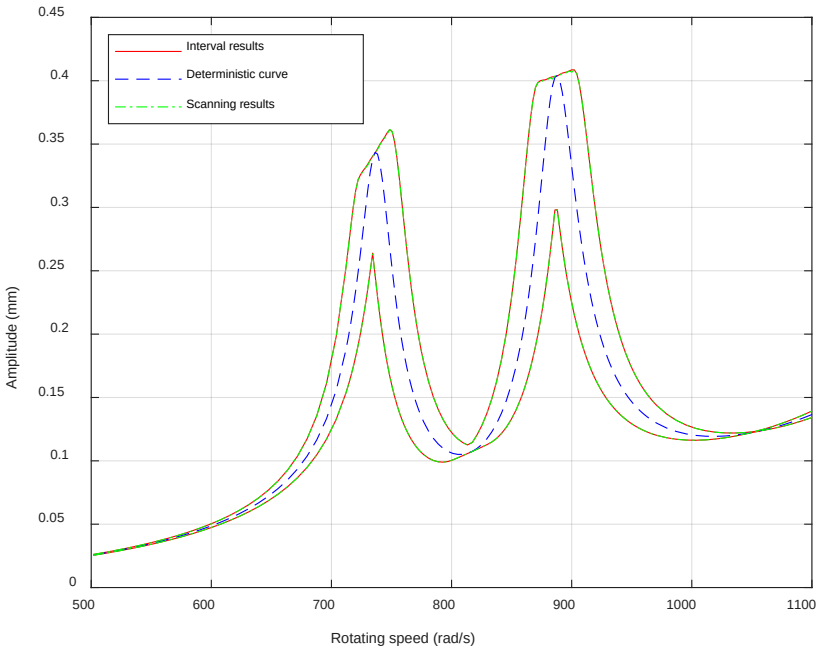

Figure 5. Dynamic response of the HP rotor with uncertain bearing stiffness.

In Figure 5, the reference solutions obtained from the conventional scanning method are also provided to verify the accuracy of the interval results. The scanning procedure generates evenly scattered samples in the uncertain parameter interval and then searches for the bounds of all the response samples. It serves as references similar to the Monte Carlo simulation in the probabilistic frame [38,39]. The 50-points reference solutions (green dotted line) plotted in Figure 5 agree well with the results obtained by the metamodel. Subsequently, the accuracy of the metamodel is validated. To obtain insight, comparisons of the vibration time histogram of the LP rotor at rotation speed 768.7 rad/s obtained from the two methods are illustrated in Figure 6. It is further demonstrated that the bounds calculated from the metamodel are in accordance with the scanning method in different time stamps. The peak shifts are observable as well. From the vibration pattern in Figure 6, we can also identify that the dynamical responses have multiple frequencies which is introduced by the multi-frequency excitations. It should be noted that, in the metamodel, only order three is used, which suggests that the deterministic model runs four times. The underlying computational cost is much lower than the scanning method. The simulations were carried out within MATLAB R2019b on a computer equipped with 16 GB RAM and Inter® Core™ i7-8550U@1.8GHz. It should be noted that the actual speed interval calculated is 0–1400 rad/s and only a part of the results are presented in Figure 5. Moreover, the increment for two consecutive speed steps is small and the initial 300 periods of the vibration are skipped for every rotational speed to eliminate the transient effects. The above conditions will cause the calculation time in a single deterministic simulation to be relatively long. However, the difference of computation time between the two methods can still show their efficiency. For the steady-state dynamical response calculations, the average CPU time elapsed in the metamodel was 28.23 min, while it was 351.87 min in the scanning method. It is shown that the computational cost needed is significantly reduced in the metamodel. The above analyses verify the accuracy and efficiency of the developed interval method in the uncertain responses prediction of the dual-rotor system.

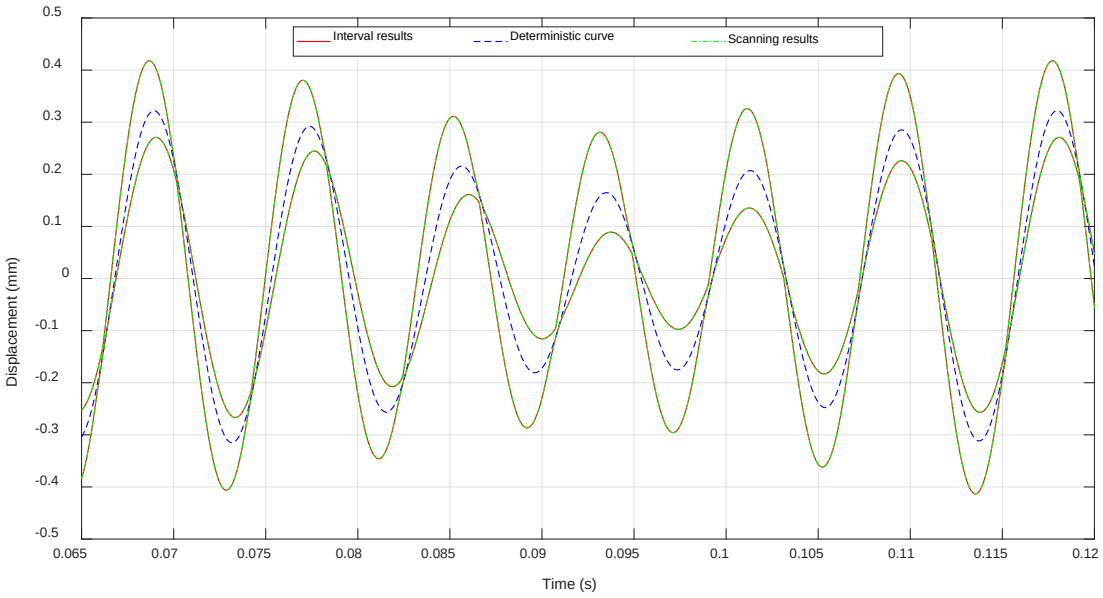

Figure 6. Time histogram of the LP rotor with uncertain bearing stiffness.

4.3. Effect of Interval Geometric Length

In this subsection, we assume the geometric length of shaft L_1 to be uncertain as a result of different assemble conditions. The uncertain degree is chosen as 10%. Figure 7 presents the interval responses of the HP rotor under uncertain shaft length. We can find that the uncertainty has influences on the whole speed range though the physical parameter is related to the inner rotor. There are trivial peak shifts as well in both resonance peaks. However, the impacts of the uncertain length are weaker than the bearing stiffness which suggests that the dual-rotor is insensitive to the length. In the speed range right after the first peak, the bounds of the response and the deterministic curve overlapped with each other. This further proves the ability of the metamodel in the prediction of the interval response of the system evidenced by the fact that the deterministic curve is rigorously enclosed in the narrow range.

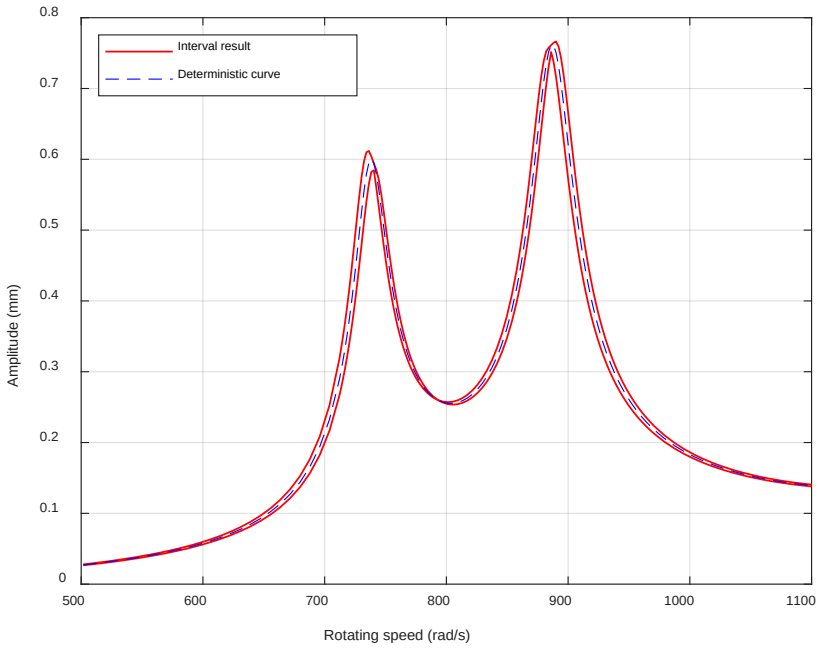

Figure 7. Dynamic response of the HP rotor with uncertain geometric length.

4.4. Effect of Multi Interval Parameters

This subsection pays attention to the influences of multi uncertain parameters [40,41] on the dynamic behaviors of the dual-rotor. Consider the uncertainties in the two imbalances and the bearing stiffness as studied in the previous subsections. The first set of uncertain degrees are 5% for the two imbalances and 2.5% for the stiffness of bearing #1. We then double their respective uncertain degrees for the second case. Figure 8 shows the results for the two cases with (a) for the HP rotor and (b) for the LP rotor. The dynamic response is significantly affected by the multiple uncertain parameters and larger uncertain degrees lead to wider response ranges. The peak shifts are observed. In the upper bounds for the HP and LP rotors, there is both a slope peak and a high-amplitude band, but the locations are switched. The slopes are also in opposite directions. These features correspond to the influence mechanism of the bearing stiffness on the two rotors since imbalances affect the vibration amplitudes linearly. We can observe a few trivial instable estimations in the upper bounds of Figure 8, which are caused by the minor errors of the metamodel as only order three is used.

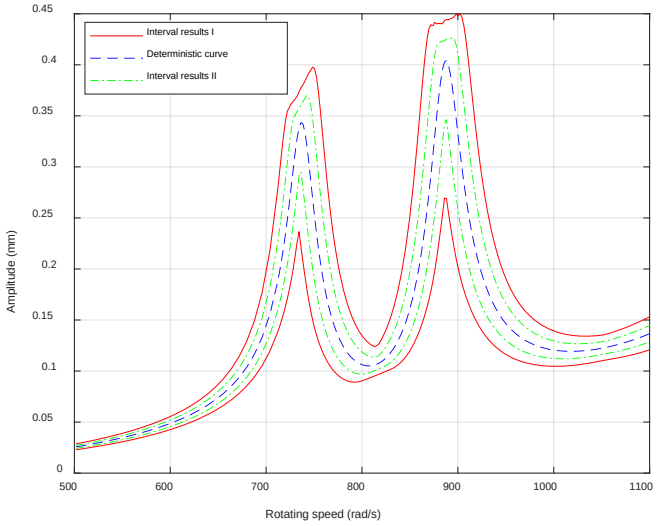

(**a**)

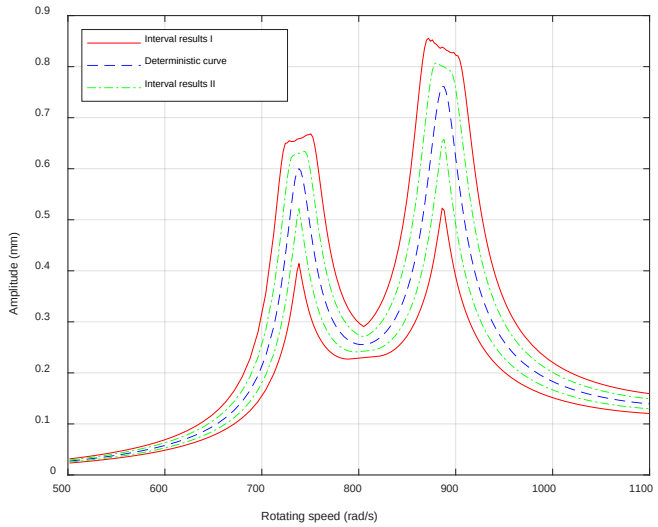

(**b**)

Figure 8. Dynamic responses of the dual-rotor with multi uncertain parameters: (**a**) Interval responses of the HP rotor; (**b**) Interval responses of the LP rotor.

In large-scale dual-rotor systems, the number of uncertain parameters that should be considered simultaneously may occasionally be very large. Although cost alleviating strategies are already incorporated, the non-intrusive metamodel used in the current research needs further improvement to cope with the exponentially growing computation burden. Alternatively, one can undertake sensitivity analyses using dedicated algorithms or investigations with individual interval parameters based on the metamodel to capture their respective contributions to the dynamical response variability and then discard those of trivial importance. Moreover, the dual-rotor system analyzed in this paper is linear. The nonlinear vibrational responses of such systems under multi interval uncertainties are much more complicated and difficult to predict, which can occur in the dual-rotors undergoing rub-impact [42], or the rotating shaft is cracked. The established method is capable of estimating the interval time history of such nonlinear vibrations. Further evaluation should be completed to verify the effectiveness of the metamodel when the steady-state frequency response has turning points.

5. Conclusions

The uncertain dynamics of a dual-rotor system under interval uncertainties are studied via non-intrusive computations. The governing motion equations are established by using the Lagrangian method. A simplex form metamodel for problems subject to single and multi-uncertain variables is constructed without modification to the deterministic solver. The calculation accuracy and efficiency are verified by the scanning method. It is found that the imbalances on the inner and outer rotors only affect speed ranges near one vibration peak. Peak shifts are observed when the bearing stiffness is considered an uncertain quantity. Moreover, the response interval of the dual-rotor is relatively small for the uncertain geometric length. These characteristics also indicate the sensitivities of the dual-rotor to the physical parameters. The multi-uncertain-variable simulations suggest that the cumulative uncertainties propagation will significantly influence the dynamics of the dual-rotor system. The main findings of this paper show some insights into the vibration characteristics of dual-rotor systems considering the non-probabilistic uncertainties.

Author Contributions: Conceptualization, C.F. and K.L.; Methodology, C.F. and J.M.; Software, G.F. and K.L.; Validation, Y.Y. and K.L.; Formal analysis, J.M. and G.F.; Investigation, K.L. and F.G.; Writing—Original draft preparation, C.F. and J.M.; Writing—Review and editing, K.L. and G.F.; Project administration, Y.Y. and F.G.; Funding acquisition, K.L. All authors have read and agreed to the published version of the manuscript.

Funding: This research was funded by National Natural Science Foundation of China, grant number 11802235 and 11972295, and Joint Doctoral Training Foundation of HEBUT, grant number 2018HW0005.

Conflicts of Interest: The authors declare no conflict of interest.

References

1. Stanković, M.; Stević, Ž.; Das, D.K.; Subotić, M.; Pamučar, D. A new fuzzy MARCOS method for road traffic risk analysis. *Mathematics* **2020**, *8*, 457. [CrossRef]
2. Roy, J.; Das, S.; Kar, S.; Pamučar, D. An extension of the CODAS approach using interval-valued intuitionistic fuzzy set for sustainable material selection in construction projects with incomplete weight information. *Symmetry* **2019**, *11*, 393. [CrossRef]
3. Gupta, K.; Gupta, K.D.; Athre, K. Unbalance response of a dual rotor system: Theory and experiment. *J. Vib. Acoust.* **1993**, *115*, 427–435. [CrossRef]
4. Yang, Y.; Cao, D.; Wang, D.; Jiang, G. Fixed-point rubbing characteristic analysis of a dual-rotor system based on the Lankarani-Nikravesh model. *Mech. Mach. Theory* **2016**, *103*, 202–221. [CrossRef]
5. Wang, N.; Jiang, D.; Behdinan, K. Vibration response analysis of rubbing faults on a dual-rotor bearing system. *Arch. Appl. Mech.* **2017**, *87*, 1–17. [CrossRef]
6. Childs, D.W. A modal transient rotordynamic model for dual-rotor jet engine systems. *J. Eng. Ind.* **1976**, *98*, 876–882. [CrossRef]
7. Zhou, H.; Chen, G. Dynamic response analysis of dual rotor-ball bearing-stator coupling system for aero-engine. *J. Aerosp. Power* **2009**, *24*, 1284–1291.

8. Hou, L.; Chen, Y.; Fu, Y.; Chen, H.; Lu, Z.; Liu, Z. Application of the HB–AFT method to the primary resonance analysis of a dual-rotor system. *Nonlinear Dynam.* **2017**, *88*, 2531–2551. [CrossRef]
9. Luo, G.; Hu, X.; Yang, X. Nonlinear dynamic performance analysis of counter-rotating dual-rotor system. *J. Vib. Eng.* **2009**, *22*, 268–273.
10. Chiang, H.W.D.; Hsu, C.N.; Tu, S.H. Rotor-bearing analysis for turbomachinery single- and dual-rotor systems. *J. Propul. Power* **2012**, *20*, 1096–1104. [CrossRef]
11. Miao, H.; Zang, C.; Friswell, M. Model updating and validation of a dual-rotor system. In Proceedings of the 26th International Conference on Noise and Vibration Engineering, KU Leuven, Leuven, Belgium, 15–17 September 2014.
12. Fu, C.; Ren, X.; Yang, Y. Vibration analysis of rotors under uncertainty based on Legendre series. *J. Vib. Eng. Technol.* **2019**, *7*, 43–51. [CrossRef]
13. Elishakoff, I.; Sarlin, N. Uncertainty quantification based on pillars of experiment, theory, and computation. Part II: Theory and computation. *Mech. Syst. Signal Process.* **2016**, *74*, 54–72. [CrossRef]
14. Soize, C. Maximum entropy approach for modeling random uncertainties in transient elastodynamics. *J. Acoust. Soc. Amer.* **2001**, *109*, 1979–1996. [CrossRef] [PubMed]
15. Fu, C.; Ren, X.; Yang, Y.; Lu, K.; Wang, Y. Nonlinear response analysis of a rotor system with a transverse breathing crack under interval uncertainties. *Int. J. Nonlin. Mech.* **2018**, *105*, 77–87. [CrossRef]
16. Ma, Y.; Wang, Y.; Wang, C.; Hong, J. Nonlinear interval analysis of rotor response with joints under uncertainties. *Chin. J. Aeronaut.* **2020**, *33*, 205–218. [CrossRef]
17. Sinou, J.J.; Nechak, L.; Besset, S. Kriging metamodeling in rotordynamics: Application for predicting critical speeds and vibrations of a flexible rotor. *Complexity* **2018**, 1264619. [CrossRef]
18. Fu, C.; Xu, Y.; Yang, Y.; Lu, K.; Gu, F.; Ball, A. Response analysis of an accelerating unbalanced rotating system with both random and interval variables. *J. Sound Vib.* **2020**, *466*, 115047. [CrossRef]
19. Yang, Y.; Wu, Q.; Wang, Y.; Qin, W.; Lu, K. Dynamic characteristics of cracked uncertain hollow-shaft. *Mech. Syst. Signal Process.* **2019**, *124*, 36–48.
20. Didier, J.; Faverjon, B.; Sinou, J.-J. Analysing the dynamic response of a rotor system under uncertain parameters by polynomial chaos expansion. *J. Vib. Control* **2012**, *18*, 712–732. [CrossRef]
21. Sinou, J.J.; Didier, J.; Faverjon, B. Stochastic non-linear response of a flexible rotor with local non-linearities. *Int. J. Nonlin. Mech.* **2015**, *74*, 92–99. [CrossRef]
22. Sinou, J.-J.; Jacquelin, E. Influence of Polynomial Chaos expansion order on an uncertain asymmetric rotor system response. *Mech. Syst. Signal Process.* **2015**, *50*, 718–731. [CrossRef]
23. Gan, C.; Wang, Y.; Yang, S.; Cao, Y. Nonparametric modeling and vibration analysis of uncertain Jeffcott rotor with disc offset. *Int. J. Mech. Sci.* **2014**, *78*, 126–134. [CrossRef]
24. Murthy, R.; Tomei, J.C.; Wang, X.Q.; Mignolet, M.P.; El-Shafei, A. Nonparametric stochastic modeling of structural uncertainty in rotordynamics: Unbalance and balancing aspects. *J. Eng. Gas Turb. Power* **2014**, *136*, 062506. [CrossRef]
25. Liu, X.; Gu, Z.; Wang, Z. Response analysis on aero-engine dual-rotor system under random excitation. *J. Propul. Tech.* **2012**, *33*, 43–46.
26. Koroishi, E.H.; Cavalini, A.A., Jr.; de Lima, A.M.; Steffen, V., Jr. Stochastic modeling of flexible rotors. *J. Braz. Soc. Mech. Sci. Eng.* **2012**, *34*, 574–583. [CrossRef]
27. Wu, J.; Zhang, Y.; Chen, L.; Luo, Z. A Chebyshev interval method for nonlinear dynamic systems under uncertainty. *Appl. Math. Model.* **2013**, *37*, 4578–4591. [CrossRef]
28. Wu, J.; Luo, Z.; Zhang, N.; Zhang, Y. A new interval uncertain optimization method for structures using Chebyshev surrogate models. *Comput. Struct.* **2015**, *146*, 185–196. [CrossRef]
29. Wu, J.; Luo, Z.; Zhang, Y.; Zhang, N.; Chen, L. Interval uncertain method for multibody mechanical systems using Chebyshev inclusion functions. *Int. J. Numer. Methods Engin.* **2013**, *95*, 608–630. [CrossRef]
30. Fu, C.; Ren, X.; Yang, Y.; Lu, K.; Qin, W. Steady-state response analysis of cracked rotors with uncertain-but -bounded parameters using a polynomial surrogate method. *Commun. Nonlinear Sci. Numer. Simulat.* **2019**, *68*, 240–256. [CrossRef]
31. Fu, C.; Ren, X.; Yang, Y.; Xia, Y.; Deng, W. An interval precise integration method for transient unbalance response analysis of rotor system with uncertainty. *Mech. Syst. Signal Process.* **2018**, *107*, 137–148. [CrossRef]
32. Hu, Q.; Deng, S.; Teng, H. A 5-DOF model for aeroengine spindle dual-rotor system analysis. *Chin. J. Aeronaut.* **2011**, *24*, 224–234. [CrossRef]

33. Sun, C.; Chen, Y.; Hou, L. Steady-state response characteristics of a dual-rotor system induced by rub-impact. *Nonlinear Dynam.* **2016**, *86*, 1–15. [CrossRef]
34. Qin, Z.; Chu, F.; Zu, J. Free vibrations of cylindrical shells with arbitrary boundary conditions: A comparison study. *Int. J. Mech. Sci.* **2017**, *133*, 91–99. [CrossRef]
35. Jacquelin, E.; Adhikari, S.; Friswell, M.; Sinou, J.-J. Role of roots of orthogonal polynomials in the dynamic response of stochastic systems. *J. Eng. Mech.* **2016**, *142*, 06016004. [CrossRef]
36. Isukapalli, S.S. Uncertainty Analysis of Transport-Transformation Models. *Diss. Theses Gradworks* **1999**, *57*, 31–32.
37. Lu, Z.; Zhong, S.; Chen, H.; Chen, Y.; Han, J.; Wang, C. Modeling and dynamic characteristics analysis of blade-disk dual-rotor system. *Complexity* **2020**, 2493169. [CrossRef]
38. Lu, K.; Jin, Y.; Chen, Y.; Yang, Y.; Hou, L.; Zhang, Z.; Li, Z.; Fu, C. Review for order reduction based on proper orthogonal decomposition and outlooks of applications in mechanical systems. *Mech. Syst. Signal Process.* **2019**, *123*, 264–297. [CrossRef]
39. Guo, X.; Ma, H.; Zhang, X.; Ye, Z.; Fu, Q.; Liu, Z.; Han, Q. Uncertain frequency responses of clamp-pipeline systems using an interval-based method. *IEEE Access* **2020**, *8*, 29370–29384. [CrossRef]
40. Zheng, Z.; Xie, Y.; Zhang, D. Numerical investigation on the gravity response of a two-pole generator rotor system with interval uncertainties. *Appl. Sci.* **2019**, *9*, 3036. [CrossRef]
41. Liu, B.; Yin, X.; Jian, K.; Wu, Y. Perturbation transfer matrix method for eigendata of one-dimensional structural system with parameter uncertainties. *Appl. Math. Mech.* **2003**, *24*, 801–807.
42. Ma, X.; Ma, H.; Zeng, J.; Piao, Y. Rubbing-induced vibration response analysis of dual-rotor-casing system. *Trans. Nanjing Univ. Aero. Astro.* **2018**, *35*, 101–108.